

# PHYSICOCHEMICAL AND BIOLOGICAL PROPERTIES OF ACHLOROPHYLL DERIVATIVE FOR PHOTODYNAMIC THERAPY IN HUMAN CHOLANGIOCARCINOMA CANCER

Tabbisa Namulinda<sup>1</sup>, Ying-Hua Gao<sup>1</sup>, Wei Zhu<sup>1</sup>, Yi-Ping Han<sup>2</sup>, Lai-Xing Wang<sup>2</sup>, Xiao-Feng Wu<sup>3</sup>, Yi-Jia Yan<sup>3</sup> and Zhi-Long Chen<sup>1\*</sup>

Department of Pharmaceutical Science & Technology, College of Chemistry and Biology, Donghua University, Shanghai, 201620, China<sup>1</sup>

Shanghai Changhai Hospital, Shanghai, 200433, China<sup>2</sup>

Shanghai Xianhui Pharmaceutical Co. Ltd, Shanghai 200433, China<sup>3</sup>

Accepted 08 September, 2017

Photodynamic therapy (PDT) is an advancing method for the treatment of cancers, and the photosensitizer is a crucial factor in the efficacy of PDT. In this study, a novel chlorophyll derivative EDPPa was synthesized by our independent laboratory. The physicochemical and biological properties were investigated. EDPPa had a characteristic long wavelength absorption at 666nm and the singlet oxygen were generated at a rate of 0.0128 S<sup>-1</sup>. In vitro, EDPPa - PDT was effective in reducing the cell viability in a drug dose-dependent and light dose-dependent manner. The confocal laser scanning microscopy demonstrated that EDPPa was distributed in the cytoplasm and nucleus of QBC-939 cells, but mainly in the lysosomes. It had obvious tumor targeting and retention in vivo and could significantly inhibit the growth of tumors after PDT and the necrotic damages were resulted. So EDPPa could be suggested as a promising anti - tumor drug candidate in PDT and in tumor fluorescent imaging or tumor diagnosis.

**Key words:** photosensitizer; photodynamic therapy; tumor; EDPPa

## 1. INTRODUCTION

Photodynamic therapy (PDT) is a promising noninvasive treatment for cancer, involving a combination of a photosensitizer and light irradiation (Szurko A et al., 2009). After irradiation with light at a specific wavelength, the photosensitizer can produce reactive oxygen species (ROS) that ultimately leads to cell death through apoptosis or necrosis (Čížeková L et al., 2014). <sup>1</sup>O<sub>2</sub> can react with many biological molecules such as DNA, lipid, free amino acids and proteins. <sup>1</sup>O<sub>2</sub> can penetrate the mitochondrial membrane or nuclear membrane, to cause DNA damage. It can also oxidize the ammonia cysteine, histidine, tryptophan and tyrosine residues. Since the photosensitizer can localize specifically within the malignant tissue, PDT displays low systemic toxicity and relative selectivity compared to chemotherapy and radio therapy (Robertson CA et al., 2009). However, the antitumor treatment of PDT has been limited by the lack of effective photosensitizers. A large number of photosensitizers have been tested in vitro and in vivo in experiments but only a few of them have been managed to reach clinical trials (O'Connor AE et al., 2009). In recent years, studies have focused on the development of new photosensitizers (Castano AP et al., 2004).

Generally, an ideal photosensitizer should have a strong absorbance with a high extinction coefficient in the long-wavelength (600 - 800 nm) region, high quantum yields for generating ROS and minimal toxicity under conditions of nonlight irradiation (Castano AP et al., 2005). The synthesis and evaluation of novel chlorophyll derivatives which exhibit these properties is presently one of the most attractive fields in research and development of photosensitizers.

Herein, a new chlorophyll derivative EDPPa was synthesized and its photodynamic activities were evaluated in vitro and in vivo.

## 2. MATERIALS AND METHODS

### 2.1 Absorption spectrum

Ultraviolet-vis absorption spectrum was carried out using an ultraviolet visible spectrophotometer (Model V-530, Japan).

Fluorescence spectrum was recorded on a Fluorescence Spectrometer (FluoroMax-4, France) in the range 550-800 nm using 411 nm excitation wavelength. All the measurements were measured at room temperature in quartz cuvettes with path length of 1 cm.

## 2.2 Singlet oxygen generation properties

The singlet oxygen quantum yields were determined using DPBF as a chemical quencher for singlet oxygen in DMF. Typically, a 3 mL portion of DMF solution containing 20  $\mu$ M DPBF and 0.5  $\mu$ M EDPPa was placed in a sealed quartz cuvette and irradiated with 650 nm light at room temperature. The absorbance of the solution at 410 nm was measured every 10 s for a 120 s period with an ultraviolet visible spectrophotometer (Zhang LJ *et al.*, 2014). The rate of singlet oxygen generation calculated by the following equation described by Wei Tang *et al.* (Tang Wei *et al.*, 2005).

$$\ln ([DPBF]_t / [DPBF]_0) = -kt$$

Where  $[DPBF]_t$  and  $[DPBF]_0$  are the concentrations of DPBF after and prior irradiation, respectively. Values of  $k$  are the rate of singlet oxygen generation and  $t$  is the time duration of irradiation.

## 2.3 In vitro photosensitizing efficacy

### 2.3.1 Cell lines and cell culture

Human cholangiocarcinoma cell QBC-939 was purchased from Chinese Academy of Sciences. The cells were cultured in RPMI-1640 medium (Invitrogen, Carlsbad, CA), supplemented with 10% fetal bovine serum (FBS, BioChrom, Cambridge, UK), 100 units/mL penicillin G (Invitrogen, Carlsbad, CA), and 100  $\mu$ g/mL streptomycin (Invitrogen, Carlsbad, CA) at 37°C in 5% CO<sub>2</sub> in a humidified incubator.

### 2.3.2 Dark and light-dependent cytotoxicity

The cells ( $1 \times 10^5$  cells/well) were seeded in 96-well micro-plates in complete medium for measurement of dark and light-dependent cytotoxicity. After 24 hr, the cells were washed once and incubated for another 24 hr with complete medium containing various concentrations of EDPPa (0, 1, 2, 4, 8, and 16  $\mu$ mol/L). All samples were handled in the dark. The cellular survival was measured with the 3-(4,5-dimethyl-2-thiazolyl)-2,5-diphenyl-2-H-tetrazolium bromide (MTT) assay. Briefly, at the end of the incubation period, 5  $\mu$ l MTT (5 mg/ml) reagent (Sigma, MO, USA) was added to each well and incubated for 4 h at 37°C. Then the medium was removed and the formazan complex was solubilized with 100  $\mu$ l DMSO. Absorbance of the complex was measured with a micro-plate reader (Bio-Rad, California, USA) at a wavelength of 570 nm.

For determination of light-induced cytotoxicity, the incubation medium was replaced with fresh medium without FCS before irradiation, and the cells were then exposed to 4 to 12 J/cm<sup>2</sup> light doses with an Nd: YAG laser (Shanghai Inter-Diff Optoelectronics Tech. China) at 650 nm. After this, the cells were incubated for 24 hr and cell viability was determined by MTT assay.

### 2.3.3 Intracellular localization

The cells were grown in six-well culture dishes on the poly-L-lysine coated cover slips, incubated at 37°C with 5  $\mu$ M EDPPa for 4 h in the dark, then washed with PBS twice and incubated with 1  $\mu$ M Lyso Tracker Blue (KeyGen, Nanjing, China) for 20 min and 1  $\mu$ g/ml Hoechst 33342 (KeyGen, Nanjing, China) for 10 min at 37°C, respectively. After washing with PBS, the cover slips were fixed for 10 min at 4°C with 4% paraformaldehyde and the cells were then examined by fluorescence with a confocal microscopy (Carl Zeiss LSM 700, Jena, Germany). EDPPa was excited with 411 nm laser and monitored at 600-700 nm.

## 2.4 In vivo experiments

### 2.4.1 Animal model

All animal procedures were approved by the Animal Care and Use Committee of Donghua University. The female Balb C nu/nu mice weighing 15 - 20 g were provided by Shanghai SLAC Laboratory Animal Company. The tumor model was established by subcutaneous injection of  $5 \times 10^6$  QBC-939 cells on the flank of rats. When tumors reached approximately 10 mm in diameter (between 21 and 28 days after tumor injection), mice were used in the following experiments.

All animals were housed individually with water and food available and quarantined for 7 days prior to initiation of the study. A 12 hr light/12 hr dark cycle (light was switched at 06:00 am) was used. Room temperature was ranged from 22°C to 27°C and the humidity was maintained between 30% and 70%.

#### **2.4.2 In vivo fluorescence imaging**

The mice model was established by subcutaneous injection of  $5 \times 10^6$  human cholangiocarcinoma QBC-939 cells with the 200  $\mu$ L PBS into the left fore limb of five-week-old male BalbC nu/nu mice. The tumors were stripped and small pieces of the tumor (approximately 1 mm square pieces) were implanted subcutaneously into the left forelimb of Balb C nu/nu mice, when implanted tumor sizes were more than 10mm in diameter. The mice were used for assay until the size of tumor reaching about 10mm.

#### **2.4.3 Bio-distribution and clearance**

The bio-distribution and clearance of EDPPa was measured in QBC-939 tumor-bearing nude mice with fluorescence measurements. Samples of heart, liver, spleen, lung, kidney, muscle, skin, brain and tumor from tumor-bearing mice were analyzed at the indicated times after injection intravenously of 20mg/kg EDPPa. Mice were sacrificed and tissue samples were obtained at different times (1, 3, 6, 12 and 24hr). The samples were placed at  $-70^\circ\text{C}$  until analysis. A 100mg tissue sample was mixed with 5 mL of ultrapure water, homogenized and centrifuged. The supernatants were collected and the fluorescence was measured with a fluorescence spectrophotometer with an excitation wavelength of 411nm and emission wavelength of 666 nm. Concentrations of EDPPa in the tissue samples were calculated from standard concentration curves, constructed by measuring the fluorescence of several different known concentrations of EDPPa.

#### **2.4.4 In vivo photosensitizing efficacy**

36 mice bearing tumors were randomized into two groups (n=18): control group without treatment and PDT group which were injected with EDPPa at a dose of 7.5 mg/kg in 0.2 mL solution via the lateral tail vein. 24hr after the injection, all animals were exposed to laser ( $\lambda=650\text{nm}$ ) with a light dose of  $100\text{J}/\text{cm}^2$ . Visible tumors were measured every 3 day using two orthogonal measurements L and W (perpendicular to L), and the volumes were calculated using the formula  $V=LW^2/2$ .

#### **2.4.5 Histology examination**

6 mice bearing tumors were randomized into two groups (n=3): control group and PDT group injected with EDPPa at a dose of 7.5 mg/kg via tail vein. For PDT group, the tumors were irradiated for 3hr with the light dose of  $100\text{J}/\text{cm}^2$  after injection. The anesthetized mice were sacrificed 30 min after irradiation. Tumors were removed and fixed with 10% neutral buffered formalin. The sliced tissues were stained with hematoxylin–eosin (H&E) and Tunel reagents, and then examined under a microscope. Tissues were examined under light microscopy by a board-certified veterinary pathologist who was blinded to treatment group.

### **2.5 Statistical analysis**

Student's T-test was used to measure differences using the Origin 9.0 software package. Data were presented as mean  $\pm$  standard deviation (S.D.) and statistical significance was taken as  $P < 0.05$ .

## **3. RESULTS AND DISCUSSIONS**

### **3.1 UV-vis and fluorescence spectra**

The UV-vis absorption, fluorescence emission spectrum of EDPPa at  $10\mu\text{M}$  was determined in DMSO and the spectra were given in Fig. 1a. Absorption spectrum of EDPPa displayed an intense Soret band at 411nm, and four less intense Q bands around 506nm, 538nm, 605nm and 661nm, respectively. Fluorescence emission spectrum of EDPPa showed a strong emission peak at 666nm and a weak fluorescence at 710nm by 411nm excitation. The emission fluorescence spectrum was shown in Fig. 1b. The results showed that EDPPa had a characteristic long wavelength absorption peak to ensure the depth of the treatment.

### **3.2 Singlet oxygen generation ability**

Energy transfer between the triplet state of photosensitizers and ground state molecular oxygen leads to the production of singlet oxygen (Çakır D et al., 2015). Since the singlet oxygen is responsible for destruction of cancer cells (Gerola AP et al., 2012), the generation ability of singlet oxygen provides important information to predict the efficiency of EDPPa in

the therapy. As shown in Fig. 1d, the absorption intensity of DPBF( $\lambda = 415\text{nm}$ ) continuously decreased in the presence of EDPPa as the irradiation time increases. The rate of singlet oxygen generation was  $0.0128\text{ S}^{-1}$ (Fig. 1c).

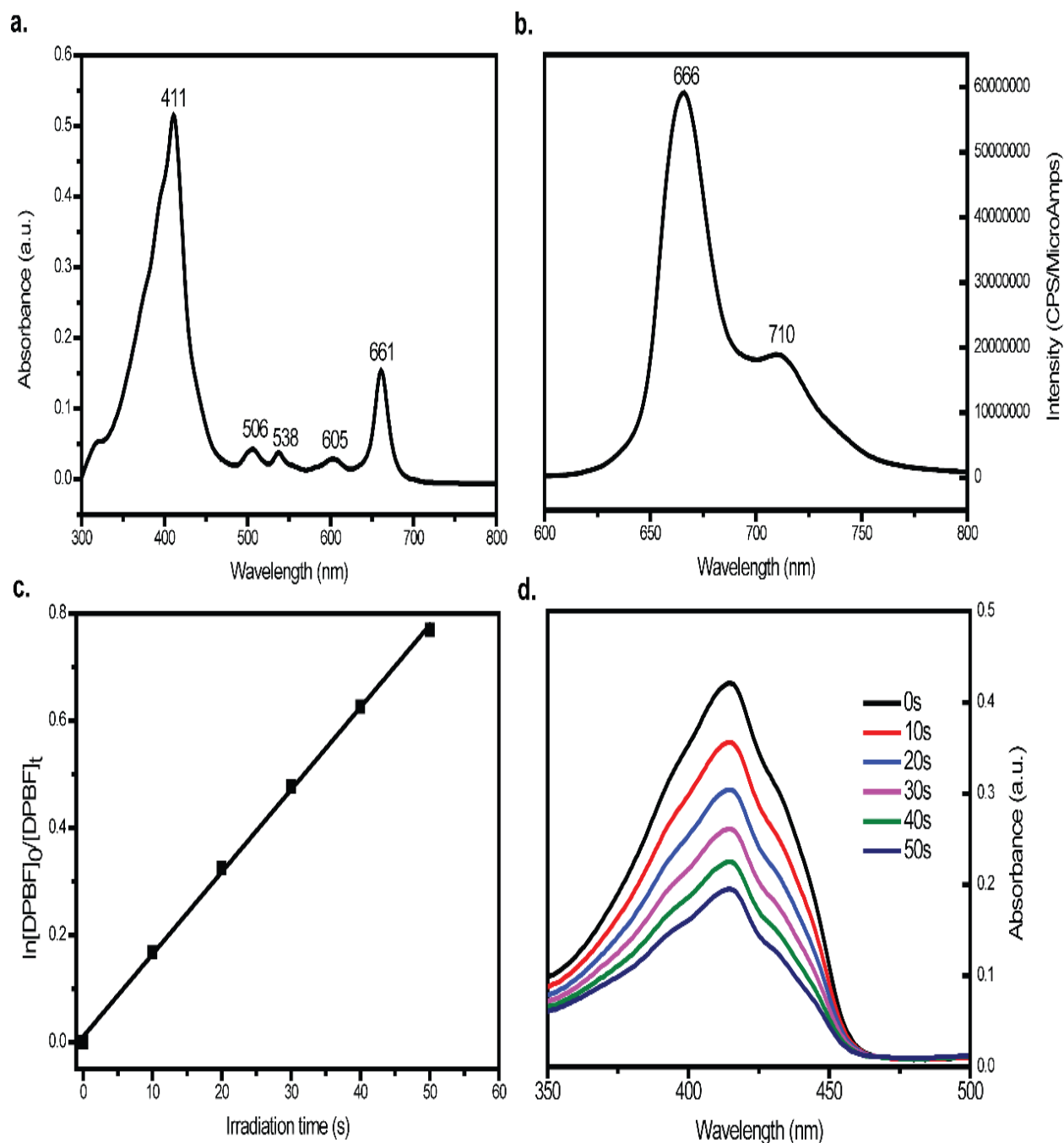


**Fig. 1** (a and b) Absorption, excitation and emission spectra for EDPPa in DMSO. Excitation wavelength = 411 nm, Emission wavelength = 666 nm. (c and d) Photodecomposition of DPBF by  $^1\text{O}_2$  after irradiation of EDPPa in DMF (monitoring the maximum absorption of DPBF at 410 nm). First-order plots for the photodecomposition of DPBF photosensitized by EDPPa.

### 3.3 Dark and light-dependent cytotoxicity

The dark and light-dependent cytotoxicity of EDPPa against QBC-939 cells were investigated using the MTT assay. In the dark, the cell viability was higher than 89% at the concentrations less than  $8\mu\text{M}$ , followed by a decrease at higher concentrations (Fig. 2). So EDPPa seems to have a slight cytotoxic effect. After irradiation with  $650\text{nm}$  laser, the cell viability decreased at the energy levels employed. The  $\text{IC}_{50}$  (the concentration of a photosensitizer inhibits 50% of the cells under light) values were shown in Table 1. The maximal reduction in cell viability was observed at  $24\mu\text{M}$  EDPPa and  $12\text{ J/cm}^2$  laser irradiation. However, considering the dark cytotoxicity,  $16\mu\text{M}$  EDPPa and  $12\text{ J/cm}^2$  might be suitable conditions for PDT.

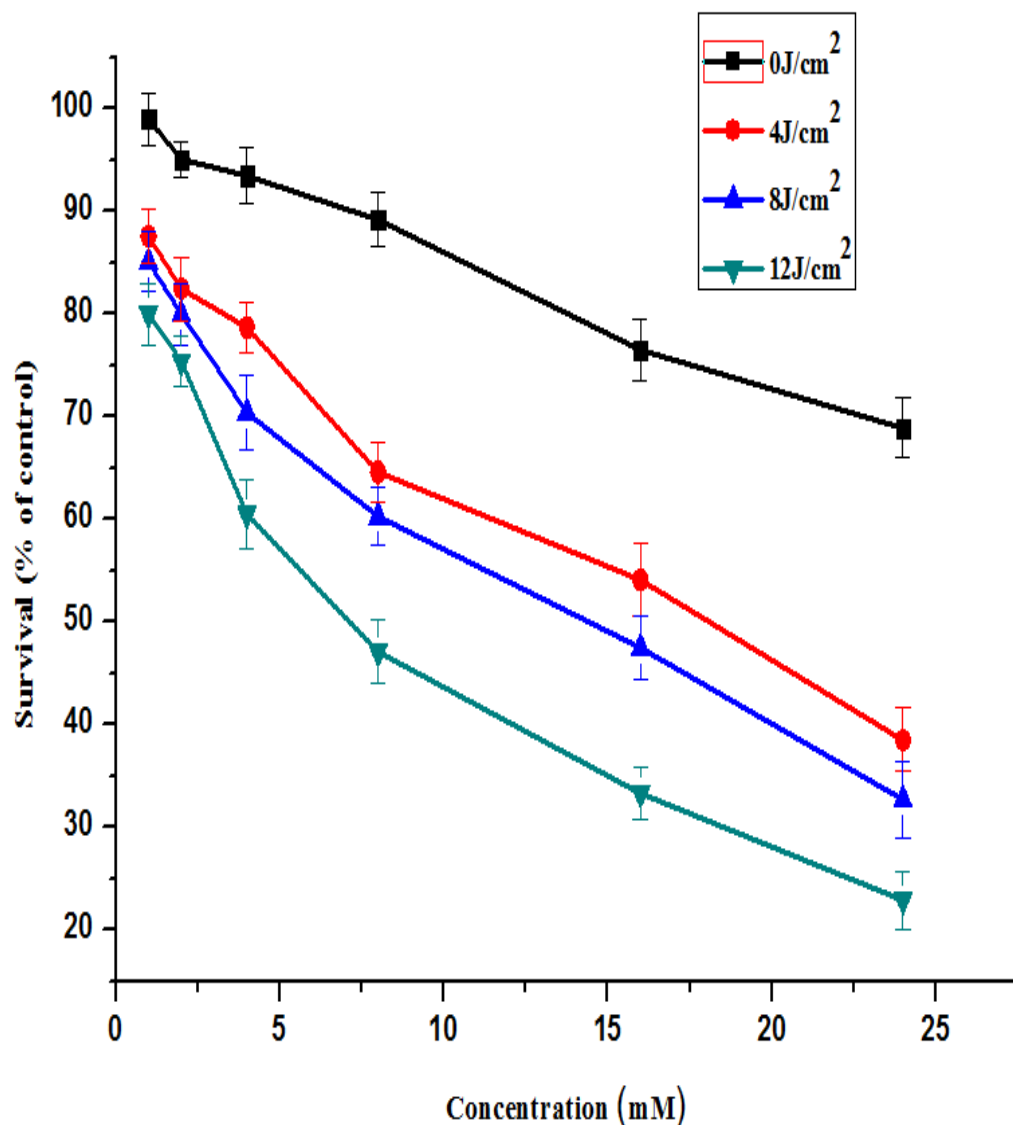


Fig. 2. Dark and light-dependent cytotoxicity of EDPPa in QBC-939 cells. Dark toxicity (0 J/cm<sup>2</sup>) of EDPPa was assessed with different concentrations (range from 0 to 12  $\mu$ M). Light-dependent cytotoxicity was assessed with different light doses (4, 8, 12 J/cm<sup>2</sup>) and different concentrations (range from 1 to 16  $\mu$ M).

**Table 1:** IC<sub>50</sub> values of EDPPa in QBC-939 cells treated for 24 h and then exposed to increasing doses of red light (650 nm).

Light doses(J/cm <sup>2</sup> )	IC <sub>50</sub> ( $\mu$ M)
4	16.79 $\pm$ 2.85
8	12.06 $\pm$ 2.13
12	6.56 $\pm$ 1.01
control (dark group)	52.38 $\pm$ 5.87

Results represent means  $\pm$  SD of three independent experiments.

\*P < 0.05 compared with control.

### 3.4 Intracellular localization

The intracellular localization of a photosensitizer is very important for its photodynamic efficacy as it determines the site of primary photo damages and the type of cellular response to the therapy(SerebrovskayaEOet al., 2011).The lysosomal localization of photosensitizer in cells also implies the involvement of apoptosis since sensitizers localized in lysosome are likely to induce apoptosis (Zheng X. et al.,2009).The confocal laser scanning microscopy images of QBC-939 cells incubated with EDPPa for 4hr were shown in Fig.3. After excitation, EDPPa emitted red fluorescence whereas that of the nucleus and lysosomes was blue. The results indicated that EDPPa was mainly localized in the cytoplasm with little accumulation in the nucleus of QBC-939 cells and targeted to the lysosomes.

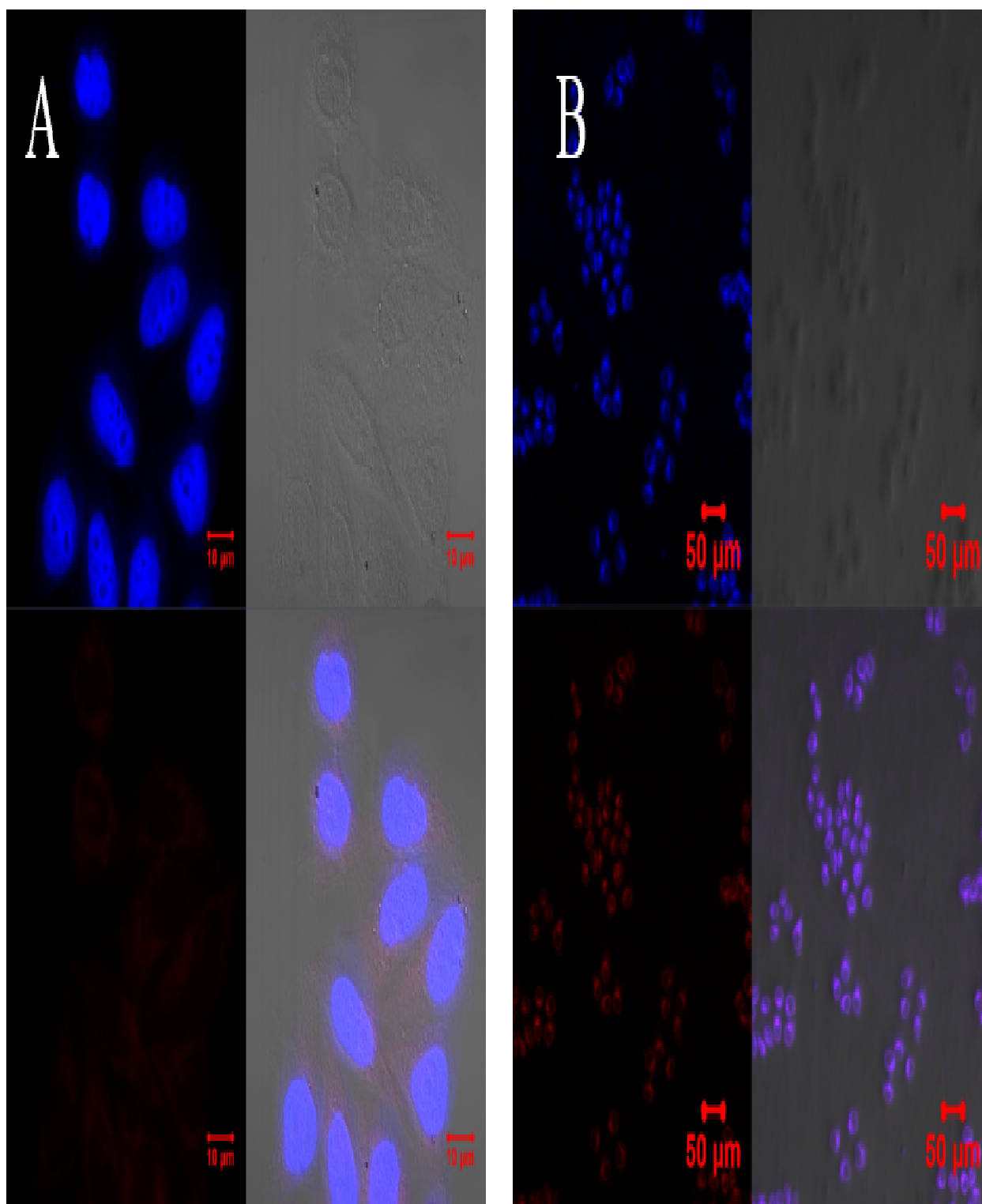
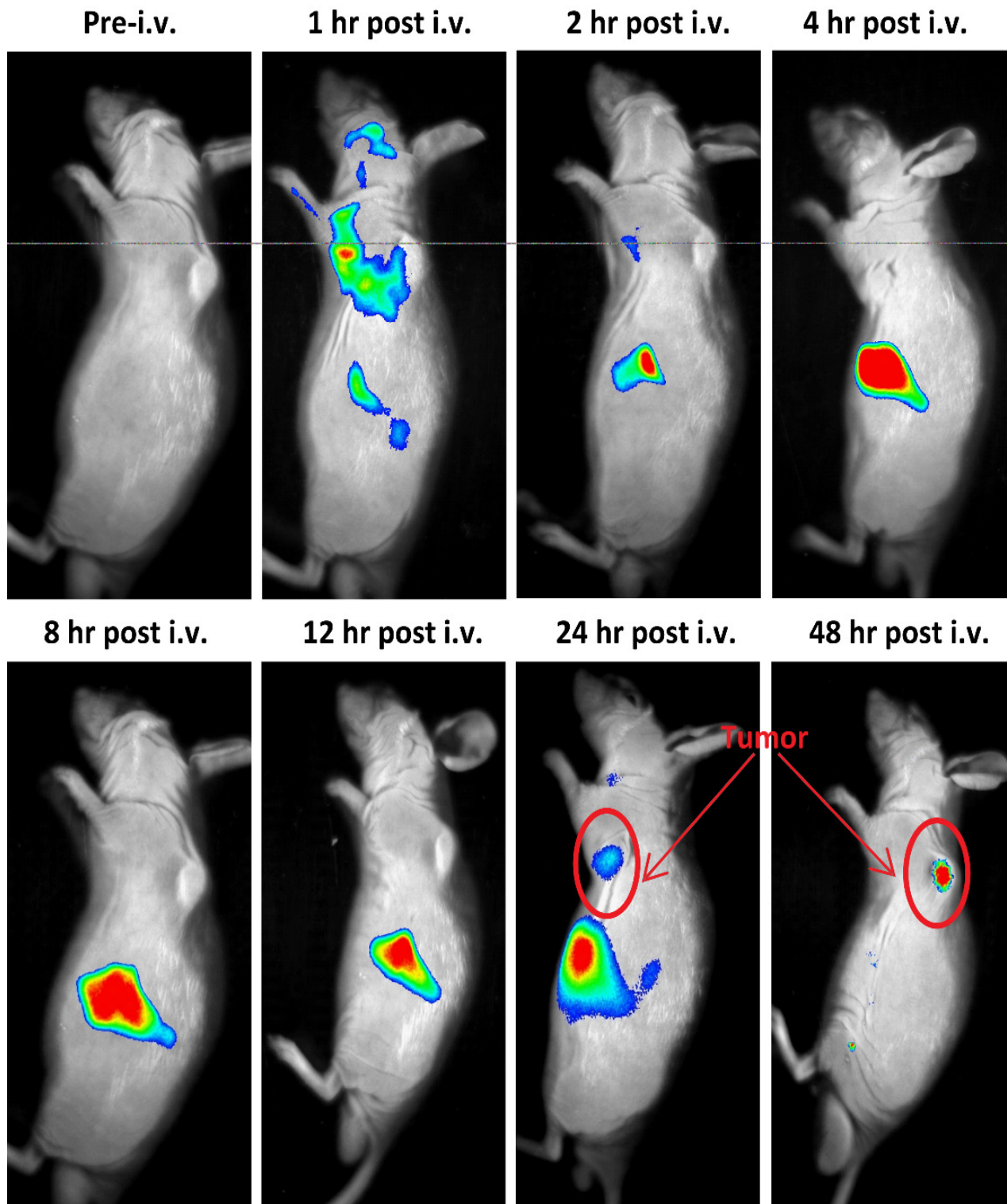


Fig. 3. The intracellular localization of EDPPa in QBC-939 cells with (A) Hoechst 33342 and (B) Lyso Tracker Blue, respectively. Images were merged to indicate the overlap in fluorescence.

### 3.5 In vivo fluorescence imaging

The mice were injected with EDPPa ( $7.5 \text{ mg kg}^{-1}$ ) by i.v. tail vein. Images were acquired at different times over the course of 48hr. EDPPa distributed in multiple tissues and organs in 1hr then gathered mainly in the liver from 2hr to 12hr by metabolic. The tumor localization was evident after 24hr with clear tumor discrimination still maintained at 48hr post administration (Fig. 4). It shows that the EDPPa had obvious tumor targeting and retention so could be used for fluorescent imaging and tumor diagnosis.



**Fig. 4.** In vivo imaging of EDPPa using a QBC-939 cholangiocarcinoma tumour model with intensity scale (excitation: 411 nm, emission: 666 nm). Circle indicates the tumour region.

### 3.6 Bio-distribution and clearance

In order to explore the distribution of EDPPa in Balb C nu/nu mice bearing QBC-939 tumor, the concentration of the drug was determined in eight tissues for time periods (1 to 24 h) after intravenous injection of 20 mg/kg of EDPPa. As shown in Fig. 5, maximum EDPPa concentrations were reached about 1hr after injection. The EDPPa concentration ratio of tumor to skin reached a maximum of 3.0 at 12hr after injection. 24hr after injection, EDPPa was eliminated from most tissues except for spleen, liver and kidney.

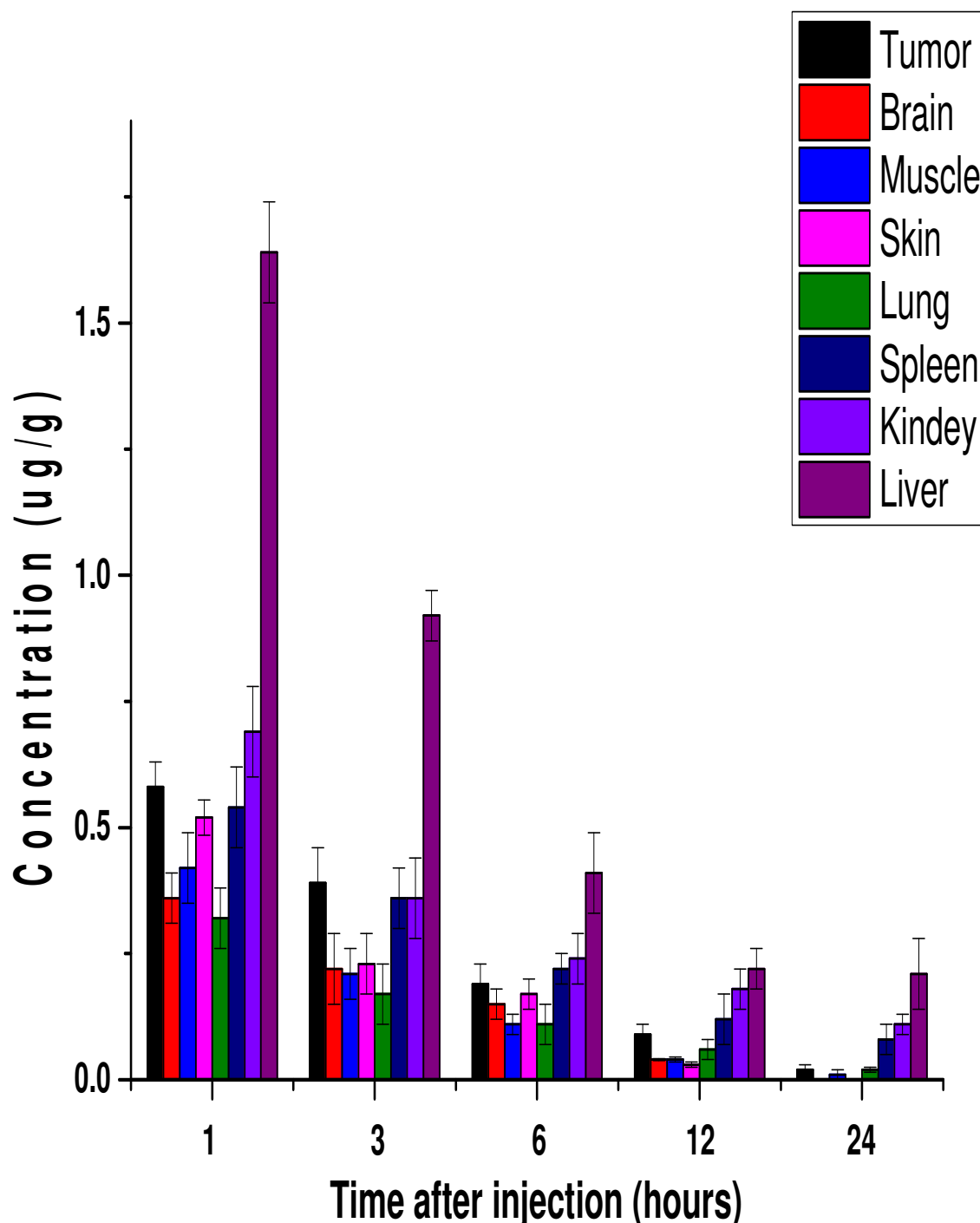


**Fig. 5.** EDPPa bio-distribution after intravenous injection (20 mg/kg) in BALB/c-mice bearing QBC-939 tumor at five different times. Eight tissues from tumor-bearing mice were analyzed. Concentrations of EDPPa in the tissue samples were determined by fluorescence measurements.

### 3.7 In vivo photosensitizing efficacy

To evaluate the in vivo PDT efficacy of EDPPa, tumor-bearing mice were injected with 7.5 mg/kg EDPPa via the tail vein, and then irradiated with 180 mW/cm<sup>2</sup> laser for 10 min (100 J/cm<sup>2</sup>,  $\lambda = 650$  nm) to the tumor area. After irradiation there was a hemorrhagic and necrotic zone in the tumor sites of PDT group. The swelling and erythema subsided within 4 days. All the tumors were measured in three dimensions every other day until 14 days. As shown in Fig. 6, tumor volumes of mice in PDT group increased more slowly compared to those of mice in control group. After 14 days, the mean size of tumors reached around 496 $\pm$ 75 mm<sup>3</sup> in PDT group, while around 1169 $\pm$ 97 mm<sup>3</sup> in control group. These indicated that EDPPa could significantly inhibit the growth of the tumors.



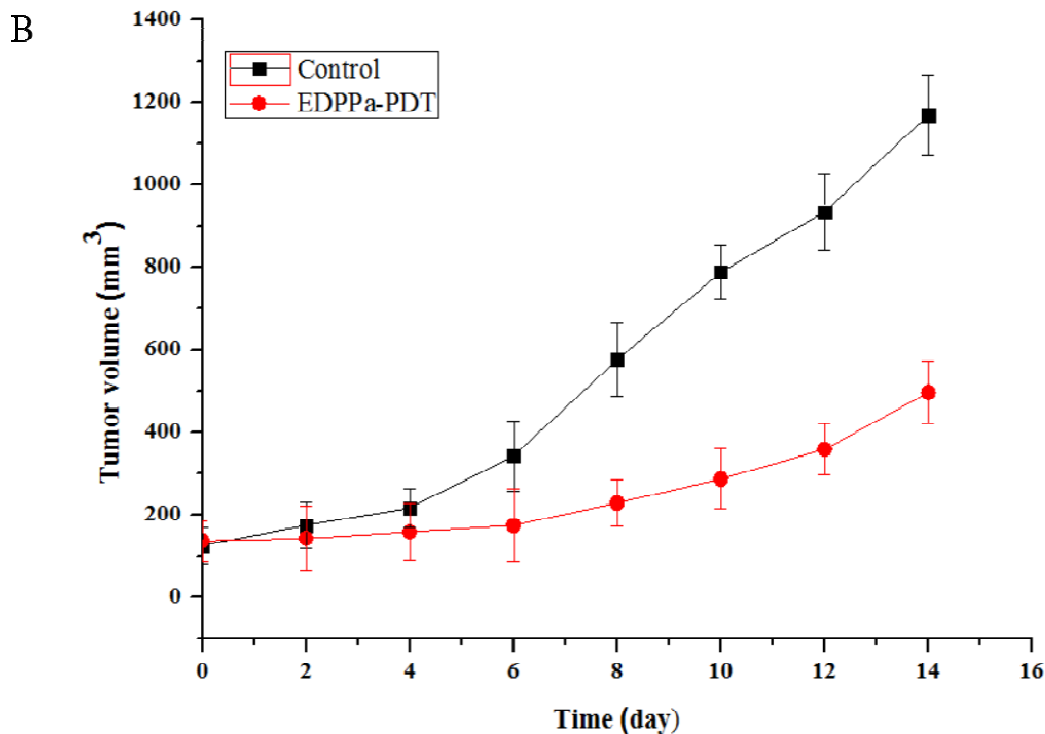
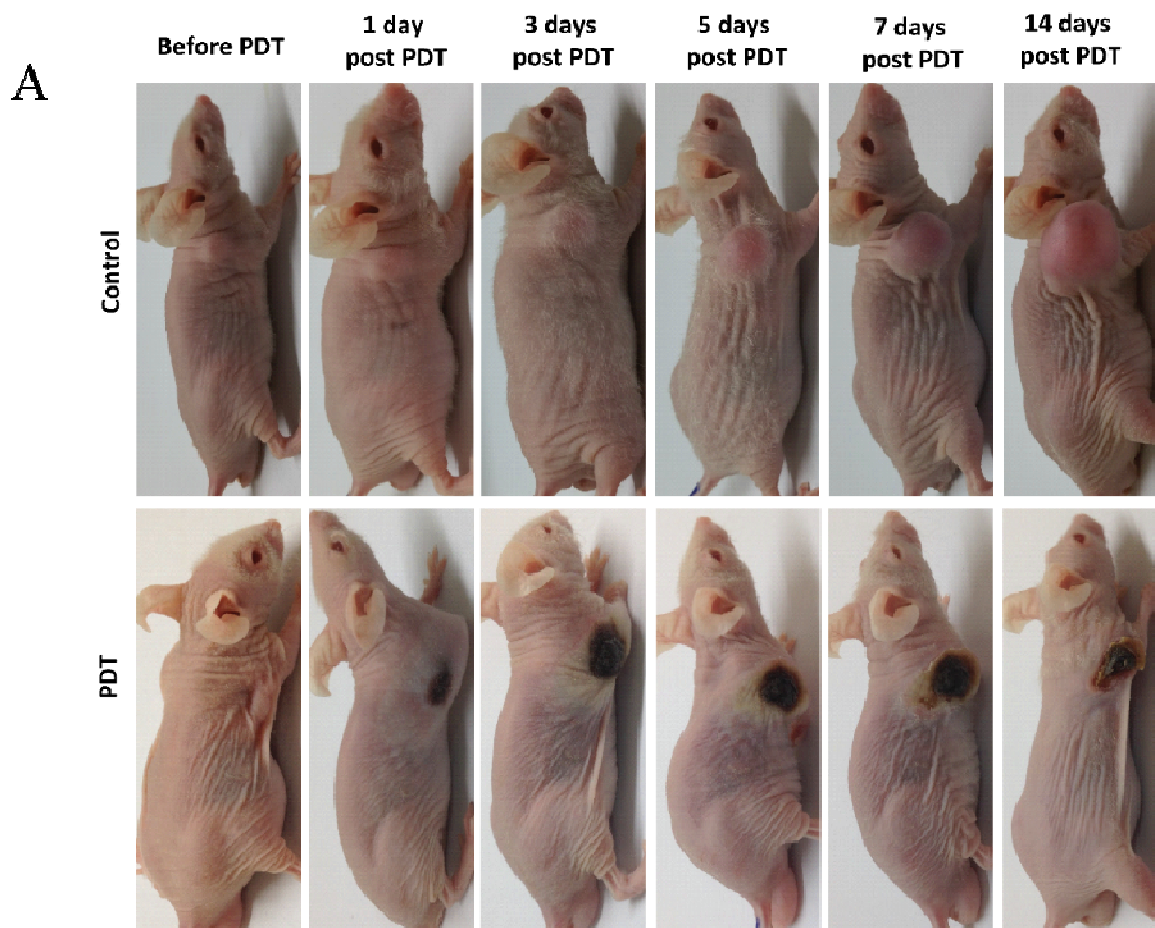
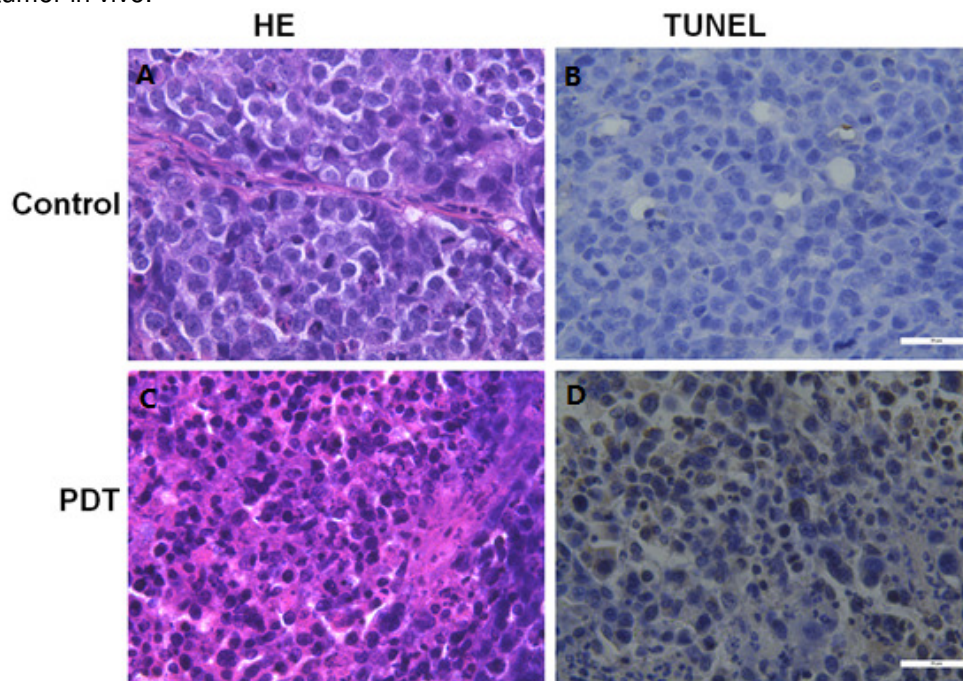


Fig.6. In vivo photosensitizing efficacy of EDPPa against cholangiocarcinoma in nude mice bearing QBC-939 tumors (18 mice/group). The mice in PDT group were treated with laser (650 nm, 100 J/cm<sup>2</sup>) at 24 h post-injection of the drug. The control mice were not subjected to any photosensitizer or light.(A). Images of tumor bearing mice before and after treatment; (B). Tumor volume at different time after treatment.

### 3.8 Histology examination

Histopathological changes were detected in cholangiocarcinoma tumors after EDPPa-PDT. After treatment, the mice were sacrificed and the tumors were removed. The tissue sections were prepared and stained with H&E and TUNEL reagents. As shown in Fig.7, necrosis and apoptosis were significantly increased in the PDT group after irradiation compared to the control group. Inflammatory cell invasion could be observed in the necrotic area. The ruptured vessel and the scattered blood cells could also be found. These results indicated that EDPPa could have inhibited the growth of tumor in vivo.



**Fig.7.** Histological examination of the QBC-939 xenograft tumors with H&E and TUNEL. Excised tumors were fixed, sectioned, and stained with hematoxylin-eosin. The sections were examined under a light microscope and photographed. H&E $\times$  400. (A, B) Control group without EDPPa; (C, D) PDT group with EDPPa.

### 4. CONCLUSIONS

In this study, EDPPa was prepared with characteristic long wavelength absorption at 666 nm. The singlet oxygen were generated at a rate of  $0.0128 \text{ S}^{-1}$  EDPPa - PDT was effective in reducing the cell viability in a drug dose-dependent and light dose-dependent manner. It could inhibit the growth of cholangiocarcinoma cells after PDT in vitro and localized on lysosomes. It had obvious tumor targeting and retention in vivo and could significantly inhibit the growth of tumors after PDT and the necrotic damages resulted. So EDPPa could be suggested as a promising anti-tumor drug candidate in PDT and in tumor fluorescent imaging or tumor diagnosis.

### ACKNOWLEDGEMENTS

This work was supported by Foundation of Science and Technology Commission of Shanghai (Grant No.17431902600, 15XD1523400, 15431904100, 17PJ1432800, 17430711900, 15411960400, 16ZR1400600), National Natural Science Foundation of China (Grant No. 21372042), the Fundamental Research Funds for the Central Universities of China (Grant No.17D110513), the Funds of Songjiang District (Grant No. 16SJGG20).

### REFERENCES

Castano AP, Demidova TN, Hamblin MR(2004). Mechanisms in photodynamic therapy. Part one: photosensitizers, photochemistry and cellular localization. *Photodiagnosis and Photodynamic Therapy*.1:279 - 293.

- Castano AP, Demidova TN, Hamblin MR(2005). Mechanisms in photodynamic therapy. Part two: cellular signaling, cell metabolism and modes of cell death *Photo diagnosis and Photodynamic Therapy*. 2:1 - 23.
- Çakır D, Göl C, Çakır V, Durmuş M(2015). Water soluble {2-[3-(diethylamino) phenoxy]ethoxy} substituted zinc(II) phthalocyanine photosensitizers for photodynamic therapy. *Journal of Luminescence*. 159: 79–87.
- Čížeková, L.Grolmusová, A.Ipóthová, Z.Barbieriková, Z.Brezová, V.Hunáková, L'Imrich, J.Janovec, L.Dovinová, I.Paulíková, H.(2014). Novel3,6-bis(imidazolidine)acridinesas effective photosensitizers for photodynamic therapy. *Bioorganic & Medicinal Chemistry*. 22:4684-4693.
- Gerola, Adriana Passarella, Semensato, Juliana, Pellosi, Diogo Silva, Batistela, Vagner Roberto, Rabello, Bruno Ribeiro, Hioka, Noboru, Caetano, Wilker(2012). Chemical determination of singlet oxygen from photosensitizers illuminated with LED: New calculation methodology considering the influence of photobleaching. *Journal of Photochemistry and Photobiology A: Chemistry*. 232:14-21.
- Ekaterrina O. Serebrovskaya, Tatiana V.Gorodnicheva, Galina V. Ermakova, Elena A.Solovieva, George V. Sharonov, Elena V.Zagay nova, Dmitriy M. Chudakov, SergeyLukyanov, Andrey G. Zaraisky, Konstantin A.Lukyanov(2011).Light-induced blockage of cell division with a chromatin-targeted phototoxic fluorescent protein. *Biochemical Journal*. 435:65-71.
- Li-Jun Zhang, Jun Bian, Lei-Lei Bao, Hai-Fei Chen, Yi-Jia Yan, Li Wang, Zhi-Long Chen(2014). Photosensitizing effectiveness of a novel chlorin-based photosensitizer for photo dynamic therapy in vitro and in vivo. *Journal of Cancer Research Clinical Oncology*. 140:1527 - 1536.
- O'Connor AE, Gallagher WM, Byrne AT(2009). Porphyrin and nonporphyrin photosensitizers in oncology: preclinical and clinical advances in photodynamic therapy. *Photochemistry and photobiology*.85:1053-1074.
- Robertson CA, Evans DH, Abrahamse H(2009). Photodynamic therapy (PDT): A short review on cellular mechanisms and cancer research applications for PDT. *Journal of Photochemistry and Photobiology B: Biology*.96:1-8.
- Szurko, Agnieszka Rams, Marzena Sochanik, Aleksander Sieroń-Stołtny, Karolina Koziolec, Agnieszka Maria Montforts, Franz-Peter Wrzalik, Roman
- Ratuszna, Alicja(2009). Spectroscopic and biological studies of a novel synthetic chlorin derivative with prospects for use in PDT. *Bioorganic & Medicinal chemistry*.17:8197-8205.
- Tang W, Xu H, Kopelman R, Philbert MA(2005). Photo dynamic characterization and in vitro application of methylene blue-containing nanoparticle platforms. *Photochemistry and photobiology*. 81:242-249.
- Xiang Zheng, Janet Morgan, Suresh K. Pandey, Yihui Chen, Erin Tracy, Heinz Baumann, Joseph R. Missert, Carrie Batt, Jennifer Jackson, David A. Bellnier, Barbara W. Henderson, and Ravindra K. Pandey(2009). Conjugation of 2-(10-Hexyloxyethyl)-2-devinylpyropheophorbide-a (HPPH) to Carbohydrates Changes its Subcellular Distribution and Enhances Photodynamic Activity in Vivo. *Journal of medicinal chemistry*. 52: 4306 – 4318.